Materials Today Bio 4 (2019) 100027

Contents lists available at ScienceDirect

Materials Today Bio

journal homepage: www.journals.elsevier.com/materials-today-bio

# Effect of peristaltic-like movement on bioengineered intestinal tube

S. Sibilio [a,d], V. De Gregorio [b,d], F. Urciuolo [a,c], P.A. Netti [a,b,c], G. Imparato [b,*]

[a] Department of Chemical Materials and Industrial Production (DICMAPI), University of Naples Federico II, P.le Tecchio 80, Naples, 80125, Italy
[b] Center for Advanced Biomaterials for HealthCare@CRIB, Istituto Italiano di Tecnologia, Largo Barsanti e Matteucci n. 53, Naples, 80125, Italy
[c] Interdisciplinary Research Centre on Biomaterials (CRIB), University of Naples Federico II, P.le Tecchio 80, Naples, 80125, Italy

ARTICLE INFO

*Keywords:*
3D engineered tubular-shaped intestine model
Air–liquid interface
Peristaltic-like motion
Extracellular matrix
Microbioreactor

ABSTRACT

The intestine is a highly heterogeneous hollow organ with biological, mechanical and chemical differences between lumen and wall. A functional human intestine model able to recreate the *in vivo* dynamic nature as well as the native tissue morphology is demanded for disease research and drug discovery. Here, we present a system, which combines an engineered three-dimensional (3D) tubular-shaped intestine model (3D In-tube) with a custom-made microbioreactor to impart the key aspects of the *in vivo* microenvironment of the human intestine, mimicking the rhythmic peristaltic movement. We adapted a previously established bottom-up tissue engineering approach, to produce the 3D tubular-shaped lamina propria and designed a glass microbioreactor to induce the air–liquid interface condition and peristaltic-like motion. Our results demonstrate the production of a villi-like protrusion and a correct spatial differentiation of the intestinal epithelial cells in enterocyte-like as well as mucus-producing-like cells on the lumen side of the 3D In-tube. This dynamic platform offers a proof-of-concept model of the human intestine.

## 1. Introduction

The human small intestine is a highly complex hollow organ located at the upper part of the intestine between the stomach and the large intestine. It is the major site of nutrient absorption. This function is facilitated by the microvilli structures lining the epithelium of the intestine. The rhythmic peristaltic motions due to smooth muscle contraction and relaxation help in food transit and increase the surface area to promote nutrient absorption. Intestinal dysfunctions can severely affect human physiology and health [1]. Three-dimensional (3D) intestinal cell culture models are currently under investigation by groups worldwide to hold the tissue engineering's promise to improve the understanding of small intestinal physiology, as well as the response of the small intestine to infection, toxicity and new therapies [2]. Furthermore, using these models may be possible to respond to the clinical demand of developing personalized intestinal tissue grafts, which can be used to repair the intestine, while avoiding the risks of immune system rejection [3]. Several biomaterial scaffolds including natural hydrogels (e.g. collagen gels and Matrigel) and synthetic scaffolds (e.g. poly–lactic-glycolic) have been investigated to provide cells a substrate for the deposition of extracellular matrix (ECM) and subsequent cell adhesion [4–6]. To mimic the tubular intestine structure, some research groups have also developed tubular porous biomaterials in which lumen the intestinal epithelial cells can be seeded and cultured to form the typical layer of polarized epithelial cells that *in vivo* featured the circular lumen of small intestine [1]. Furthermore, the pre-epithelialized scaffolds have been often cultured in bioreactor systems for dynamic cultivation allowing longer term investigation and studies of microbiome–intestine interactions [1, 7–9]. In other approaches, porous hollow fibre bioreactors have been used to accelerate the differentiation process of Caco-2 cells toward enterocytes phenotype by exploiting both the tubular morphology resembling the lumen of the human small intestine and the dynamic environment of the bioreactor system [10]. However, as it is widely reported, the morphogenesis of the complex architecture of tubular organs is a highly dynamic process that involves the reciprocal signalling between epithelium and the mesenchyme that in turn involves cell migration, polarization, shape changes, adhesion to neighbouring cells and the ECM remodelling [8]. In the scaffold-based approaches, the intestinal epithelial cells are lined on a surrogate of the intestinal ECM that fail in faithfully reproducing the spatiotemporal signal presentation of the native mucosal lamina propria and the correct

* Corresponding author.
*E-mail address:* giorgia.imparato@iit.it (G. Imparato).
[d] These authors contributed equally to this work.

https://doi.org/10.1016/j.mtbio.2019.100027
Received 6 May 2019; Received in revised form 5 August 2019; Accepted 1 September 2019
Available online 19 September 2019

epithelia–mesenchyme cross-talk that *in vivo* regulate morphogenetic processes [1,11,12]. Recent technical advances in the stem cell field have enabled the *in vitro* generation of intestinal organoids that offer the possibility to support differentiation of various intestinal epithelial cell subtypes and to study the villus morphogenesis *in vitro* [13]. However, they are also limited in that they lack the luminal accessibility impairing the possibility to sample or manipulate luminal components (i.e. microbial species or drugs) and do not experience fluid flows and cyclical mechanical strain so failing in reproducing the *in vivo* physiological microenvironment [14]. The last years have also saw the birth of several gut-on-a-chip micro devices to mimic the dynamic motion of the human small intestine, to allow the manipulation of luminal component as well as the possibility to study many critical intestinal functions (e.g. absorption, permeability, transepithelial electrical resistance) [7]. However, the overly simplicity of cellular models in such microfluidic device, impair to recapitulate the spatial and chemical complexity of living tissues and cannot approximate correctly neither the pathophysiological events nor the developing tissue. Here, we present a 3D-engineered tubular-shaped intestine tissue (3D In-tube) with a completely endogenous scaffold-free ECM, cultured in a custom-made microbioreactor to induce a peristalsis-like stimulation on the serosal side of the 3D In-tube. We have previously demonstrated that both the composition and the architecture of the intestinal stroma equivalent strongly influence the intestinal epithelium morphogenesis and its function [15,16]. Here, we adapted the previously established bottom-up tissue engineering approach [15] to produce the 3D tubular-shaped lamina propria. In addition, we designed and developed a handy custom-made glass microbioreactor capable to induce the serosal stimulation as well as the air–liquid interface (ALI) culture in dynamic condition. We demonstrated, for the first time, the spontaneous production of villi-like protrusions and a correct spatial differentiation of the intestinal Caco-2 epithelial cells in enterocytes and mucus-producing cells in the lumen side of a tubular-shaped intestine tissue. This innovative platform overcomes the limitations of the aforementioned intestinal models providing a more reliable tool for *in vitro* studying the passage and absorption of luminal content in pathophysiological conditions, as well as for *in vivo* transplantation to replace the intestinal damaged tissue.

## 2. Materials and methods

### 2.1. Preparation of porous gelatin microbeads

Gelatin porous microbeads (GPMs) have been prepared according to a modified double emulsion technique (O/W/O). Gelatin (type B Sigma Aldrich Chemical Company, Bloom 225, Mw 1⁄4 176,654 Da) was dissolved into 10 mL of water containing TWEEN 85 (6% w/v) (Sigma Aldrich Chemical Company). The solution was kept at 60 °C. Toluene containing SPAN 85 (3% w/v) (Sigma Aldrich Chemical Company) was continuously added to the aqueous gelatin solution (8% w/v) to obtain primary oil in water emulsion. The added toluene formed droplets in the gelatin solution until saturation. Beads of gelatin containing droplets of toluene were produced through the addition of excess toluene (30 mL) that allowed for a double emulsion (O/W/O). After cooling below 5 °C, 20 mL of ethanol were added to extract toluene and stabilize GPMs. The resulting microspheres were filtered and washed with acetone and then dried at room temperature (RT). Microspheres were separated selectively by using commercial Sieves (Sieves IG/3-EXP, Retsch, Germany). GPMs with 75–150 μm size range were recovered and further processed. After sieving, the number of GPM per milligram was determined by counting microbeads in a cell culture dish (w/2 mm grid Nunc). The number of dry microcarriers per milligram was determined to be $5*10^3$ beads/mg and was evaluated to control the cell/microcarriers ratio at the inoculum step of the spinner culture. Before their use, dry GPMs were sterilized with ethanol 100% for 24 h, then washed thrice in phosphate-buffered saline (PBS) (0.1 M). Before cell seeding, PBS was removed and replaced with culture medium.

### 2.2. Spinner flask cell culture

Human intestinal myofibroblasts (H-InMyoFibs) were purchased from Lonza and cultured in SMGMTM-2 BulletKitTM medium (Lonza). Cells were cultured in T-150 $cm^2$ tissue culture flasks (Corning), maintained at 37 °C, 5% $CO_2$ humidified atmosphere and harvested with 0.25% trypsin-EDTA (Gibco) before seeding. H-InMyoFibs at 3–5 passage were used. The microbeads/myofibroblasts cultures were propagated in spinner flasks (13 cells/beads) (100 mL, Belco) for 10 days, to obtain InMyoFib-microtissue precursors (InMyoFib-μTPs), was stirred intermittently at 10 rpm (5 min stirring and 40 min static incubation) for the first 6 h after inoculation to allow cell adhesion, and then continuously at 20 rpm for up to 10 days. The spinner cultures were incubated at 37 °C in 5% $CO_2$ and the medium was changed every 2 days.

### 2.3. Cell/microbeads counting

To obtain cell/microbeads ratio, 1 mL aliquots of InMyoFib-μTPs were collected at different culture days of dynamic cell seeding (0, 3, 6 and 10 days). Briefly, three aliquots of 200 μL each were transferred to a cell culture dish (w/2 mm grid Nunc) for microcarrier counting by using an optical microscope (BX53; Olympus). Then, the suspension was harvested in a new 1.5 mL tube, washed twice with PBS and digested by Collagenase A at 2.5 mg/mL (Roche) at 37 °C for 45 min until the scaffold was completely dissolved. The detached cells were then counted using a haemocytometer and the cell per bead ratio was evaluated.

### 2.4. Histological, immunofluorescence and multiphoton imaging of InMyoFib-μTPs

InMyoFib-μTPs were fixed in a 10% neutral buffered formalin solution for 1 h, rinsed in PBS, dehydrated in an incremental series of alcohol (75%, 85%, 95% and 100% twice, each step 30 min at RT), then treated with xylene (30 min twice) and embedded in paraffin. Tissue sections, 5 μm thick, were stained with haematoxylin and eosin (H/E), mounted on coverslips with Histomount mounting solution (Bioptica) and observed with a light microscope (Olympus CK 40). For immunofluorescence and second-harmonic generation (SHG) imaging, 1 mL aliquots of InMyoFib-μTPs were taken at 10 days from the spinner culture and were processed. The unstained samples were fixed with 4% paraformaldehyde for 20 min at RT, permeabilized with 0.1% triton for 10 min and blocked with 3% bovine serum albumin (BSA; Sigma Aldrich) for 50 min. Then, samples were incubated with primary antibodies for alpha smooth muscle actin (α-SMA) (1:500; Abcam) overnight at 4 °C, washed extensively and incubated with a 1:500 dilution of fluorescent secondary antibody (546 Alexa fluor, Termofisher) at RT for 1 h. InMyoFib-μTPs were rinsed, and counterstained with 4′,6-diamidino-2- phenylindole (DAPI) (Sigma Aldrich) at dilution ratio (1:10000 in PBS) for 10 min. Samples incubated with dilution buffer without primary antibody were used as a negative control. Images of the stained samples were obtained using confocal laser scanning microscopy. Moreover, two-photon–excited fluorescence has been used to induce SHG and obtain high-resolution images of unstained collagen structures of InMyoFib-μTPs' ECM. The samples were also observed to highlight the simultaneous excitation of the two different fluorophores used (Dapi $\lambda_{ex}$ 810, $\lambda_{em}$ 910 nm; α-SMA $\lambda_{ex} = 540–545$ nm, $\lambda_{em} = 570–573$ nm) as well as to induce SHG ($\lambda = 840$ nm).

### 2.5. 3D tubular stroma formation

InMyoFib-μTPs suspension was transferred by pipetting into an opportunely designed assembling chamber to allow their moulding in 1-mm-thick planar stroma (circle 3 cm diameter) [14]. During the filling procedure, no bubble formation was assured into maturation chamber,

which was closed and placed on the bottom of a spinner flask completely covered by culture medium. The spinner worked at 60 rpm and the medium was exchanged every 2 days and 2-O-alpha-D-glucopyranosyl--L-ascorbic acid 0.5 mM (TCI Europe) was added at every medium exchange. After 2 weeks of culture, disk-shaped planar stroma was rolled around a cylindrical stainless steel net long 2.5 cm and having a diameter of 0.5 cm (Fig. 1A and B) and accommodated in stainless steel cylinder (Fig. 1C) and cultured for 2 weeks in a spinner flask to obtain a 3D tubular stroma.

### 2.6. Bioreactor design for 3D In-tube formation

To produce the 3D In-tube, intestinal epithelial cells were seeded on the luminal side of the 3D tubular stroma (Fig. 2A). To this aim, 3D tubular stroma was rinsed with three washes of PBS solution (0.1 M) and allowed to dry for 5 min under laminar flow. Subsequently, 500 μL of the Caco-2 suspension ($1 \times 10^4$ viable cells/cm$^2$) was seeded in the luminal side of the 3D tubular stroma in two rounds where the 3D tubular stroma was rotated at 180° in the first seeding round (Fig. 2B). An incubation period of 30 min was allowed between the seeding steps. Then, the sample was incubated for at least 2 h in incubator at 37 °C with 5% $CO_2$ to allow the complete cell seeding into the 3D tubular stroma. The medium was added until the sample is completely submerged, this condition promotes the Caco-2 horizontal spreading. Submerged culture lasted approximately 2 days. Then, an optimized ALI culture lasting 10 days took place to induce the epithelial tissues to differentiate. A custom-made glass microbioreactor was designed to culture 3D In-tube in ALI culture and to induce, by modulating flow rate, shear stress reproducing the intestinal peristalsis movement [15] on the external side of 3D In-tube. The external chamber of the microbioreactor was composed by a cylindrical glass chamber (PYREX® Roller Bottles, 100 mL) and 2 polydimethylsiloxane (PDMS) (10:1 w/w; Sylgard 184, Dow Corning) caps. The cylindrical glass custom-made chamber presented a diameter of 2.5 cm and a height of 6.5 cm. Pyrex was used for the following main reasons: firstly, it allows sterilization by autoclave; secondly, it is optically accessible allowing visual inspection during culture time. To connect the external chamber to the fluid-dynamic circuit, two PDMS cups containing connectors were fabricated as follows: two cylindrical connectors (Harvard apparatus; Male Luer Taper ¼ in inner diameter, Polypropylene) were positioned on the bottom of two beakers containing liquid PDMS (PYREX Glass Beaker, 30 mL). After curing for 2 h at temperature of 65 °C, PDMS solidified and entrapped the connectors. This procedure was used to fabricate two rubber-like connectors that could easily sealed to the opened sides of the external chamber. The microbioreactor, tubes (Tubes Tygon® E-LFL, 0.125 in; inner diameter) and connectors were sterilized by autoclaving. The 3D In-tube edges were plugged in other two cylindrical hollow connectors (Harvard apparatus; Male Luer Taper 1/8 in inner diameter, Polypropylene) and further sealed with 5 mg/mL collagen gel (Ibidi, Collagen Type I, rat tail), neutralized by dropwise addition of 0.1 g NaOH and placed in an incubator at 37 °C for 45 min to allow the collagen polymerization (Fig. 2C). Then, a long needle (BD Microlance, hypodermic needle, 0.4 mm inner diameter 19 mm length) was inserted into the hollow of the cylindrical support and was linked with PDMS caps of both sides to constrain the 3D In-tube into the microbioreactor and to ensure the ALI culture. The microbioreactor was connected to peristaltic pump (Ismatec™ MS-4/12 Reglo Digital Pump) set at a flow rate of 8 mL/min. To reproduce peristaltic-like motion wave, we set peristaltic pump interval pause of 0.5 s every 2 s of normal dispensing fluid flow, obtaining the square wave reported in the Fig. 3A. The entire final morphology of the 3D In-tube was observed by using microcomputed tomography (micro—CT; X-Ray Micro-Computed Tomography Skyscan 1172, Bruker, Germany) and the inner surface of the 3D In-tube was explored with stereo microscope (Camera Leica IC80HD on EM UC7 Leica Microsystems, Germany). At the end of the experiments, the 3D In-tube was collected and processed for histological (H/E), immunofluorescent and ultrastructural analyses.

### 2.7. COMSOL multiphysics (computational fluid dynamic)

#### 2.7.1. Governing equation

A computational fluid dynamic (CFD) simulation study on bioreactor for 3D In-tube was carried out by means of COMSOL Multiphysics, version 5.0, to define the velocity and the oxygen concentration profile during the perfusion culture. The system was divided in two different domains as shown in Fig. 3B, a fluid domain indicated with "*f*", which identified the region filled with culture medium, and a tissue domain, indicated with "*t*", which identified the region filled with the intestinal tissue equivalent. To model the oxygen transport according to the normal convection—diffusion equation, a coupling of laminar flow and transport of diluted species interfaces has been set, assuming that the oxygen is very diluted compared with water. In our model, we considered the intestinal tissue equivalent inside the bioreactor as a porous media. The Navier—Stokes Eq. (1) was used to describe the fluid flow in the fluid domain:

$$\mu^f \nabla^2 v^f = \nabla P^f \tag{1}$$

where $\mu^f$ is the dynamic viscosity, $v^f$ is the fluid velocity and $P^f$ is the pressure. The transport in the tissue domain was described by using slow flow in porous media or Brinkmann Eq. (2):

$$\frac{\rho}{\varepsilon\left(\frac{(v\cdot\nabla)v}{\varepsilon}\right)} = \nabla\cdot\left[-pI + \frac{\mu^t}{\varepsilon}\left(\nabla v + (\nabla v)^T\right) - \frac{2\mu^t}{3\varepsilon}(\nabla v)I\right] - \left(\mu^t K^{t-1} + \beta|v|\right) + F \tag{2}$$

where $K^t$ is the hydraulic permeability, $\mu^t$ is the effective viscosity of the fluid in the tissue domain, $F$ represents the body forces, $p$ is the pressure and $v$ is the fluid velocity field. Transport of diluted species was used to

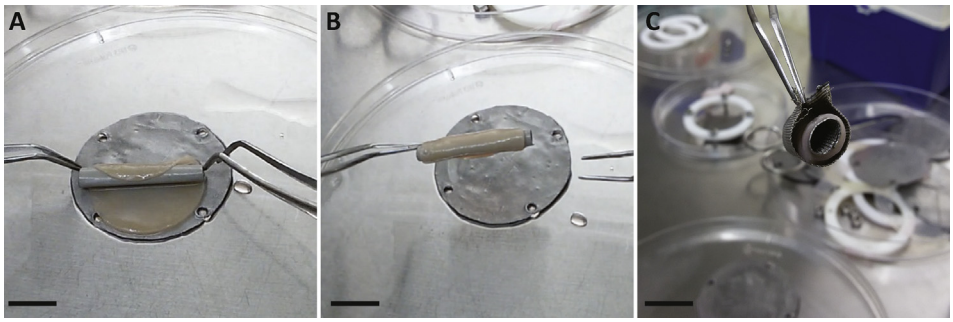


**Fig. 1.** Human intestinal stroma formation in a tubular-like shape. A) Rolling of three-dimensional (3D) planar stroma around a cylindrical stainless steel of 0.5 cm in diameter, scale bar 2 cm; B) 3D planar stroma just wrapped around the cylindrical stainless steel, scale bar 0.5 cm and C) image of 3D tubular stroma accommodated in stainless steel cylinder for dynamic culture, scale bar 0.5 cm.

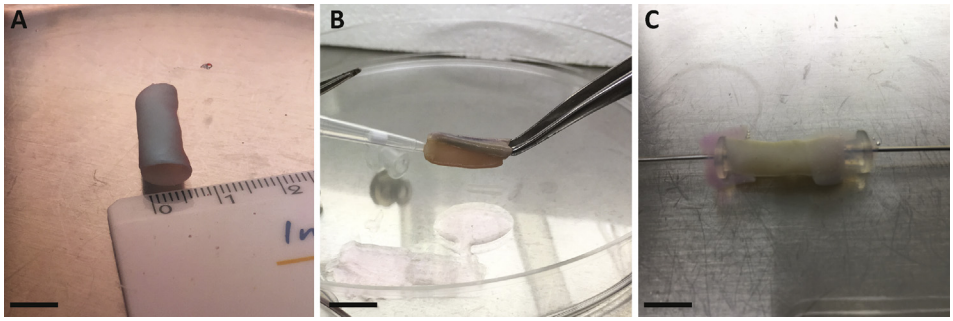


**Fig. 2.** Caco-2 seeding in 3D tubular stroma. A) Image of 3D tubular stroma 1-mm-thick after 42 weeks of dynamic culture, scale bar 0.6 cm; B) Caco-2 cell seeding in the luminal side of the 3D tubular stroma, scale bar 2.5 cm and C) sealing of 3D In-tube with collagen gel for air–liquid interface (ALI) culture, scale bar 0.8 cm.

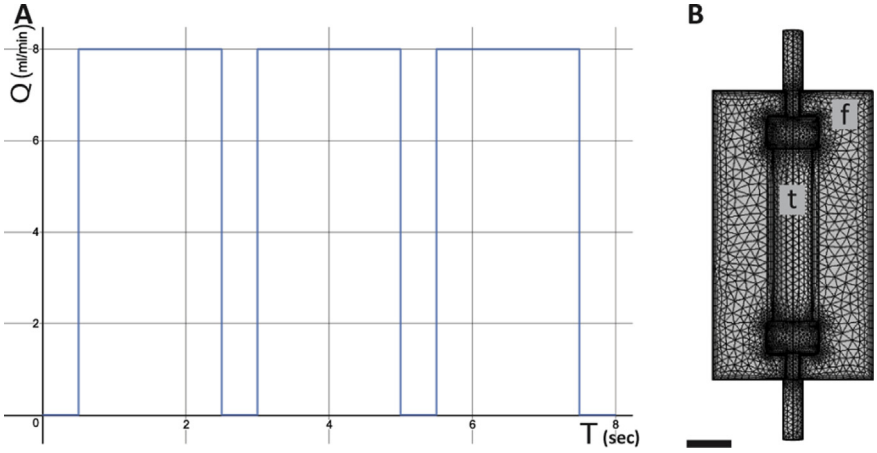


**Fig. 3.** Bioreactor system and peristaltic-like wave. A) Square wave reproduced by peristaltic pump set at a flow rate of 8 mL/min and B) computer aided design (CAD) and mesh of the bioreactor system for 3D In-tube ALI culture used for computational fluid dynamic (CFD) simulation, "f" indicates the fluid domain and "t" identifies the tissue domain, scale bar 2 cm.

describe the oxygen consumption by the intestinal tissue equivalent inside the chip by using the following mass balance Eq. (3):

$$D\nabla^2 C - \nabla(Cv) = -R \tag{3}$$

where $C$ is the oxygen concentration, $v$ is the fluid velocity field that was set equal to $v^f$ in the domain "$f$" and to $v^t$ in the domain "$t$". $D$ is the diffusion coefficient of the oxygen, set as $D^f$ in the domain "$f$" and as $D^t$ in the domain "$t$". $R$ *is* the volumetric oxygen consumption rate expressed by the Michaelis–Menten law according to the following Eq. (4):

$$R = \rho \frac{V_{\max} C}{K_m + C} \tag{4}$$

where $V_{max}$ is the maximum oxygen consumption rate and $K_m$ is the concentration at which the oxygen consumption rate is half of $V_{max}$, $\rho$ is the cell density in the perfusion chamber obtained by considering the number of cells of intestinal tissue in the bioreactor for 3D In-tube device. $R$ was set to 0 only in the fluid domain, because cells are included only in the tissue domain. All the variables used in the simulation are reported in detail in Supplementary Table S1.

### 2.7.2. Boundary conditions

The boundary conditions were set as follows:

$v^f = \frac{Q_{in}}{A}$; $C = C_0$ at the inlet $P^f = 0$; $C = C_0$ at the outlet.

$P^f = P^t$; $v^f = v^t$; $J^f = J^t$ at the interface of the $f/t$ domains.

Where $Q_{in}$ *is the*imposed flow rate at the inlet (8 mL/min) and J is the total (convention + diffusion) oxygen flux;

$v = 0$; $J = 0$ at the boundaries.

All the values used in the simulation are present in Table 1.

### 2.8. Cell toxicity test

To evaluate the cell viability, the culture media supernatants from each spinner flask were collected for lactate dehydrogenase enzyme (LDH) release every 3 days up to the 42$^{nd}$ day and stored at −20 °C before being analyzed. Specifically, LDH activity was measured from day 3 to day 10 during spinner culture time and from day 15 to day 42 in maturation chamber. LDH release was quantified by using an LDH Assay Kit (Sigma Aldrich) according to the manufacturer's instruction by using the following equation:

$$LDH = (B \times Sample\ dilution\ factor)/\text{Reaction time} \times V$$

**Table 1**
Values of the variables used in the mathematical modelling.

| Description [Symbol] | Value [Unit] |
|---|---|
| Equilibrium oxygen concentration in the culture media [$C_0$] | 0.22 [μM] |
| Cell per $\mu TPs$ [$\rho_{HD}$] | $0.2 \times 10^{14}$ [cell/m$^3$] |
| Maximum rate of oxygen consumption [$V_{max}$] | $2.2 \times 10^{-5}$ [μmol (cell s)$^{-1}$] |
| Oxygen concentration at $\frac{V_{max}}{2}$ [$K_m$] | 0.001 [mol/m$^3$] |
| Dynamic permeability [$\kappa_{dv}$] | 0 [m$^2$] |
| Source term [Q] | 0 [kg/m$^3$/s] |
| Dynamic viscosity of the culture media [$\mu^f$] | 0.001 [Pa s] |
| Effective viscosity in the fluid [$\mu^t$] | 0.0016 [Pa s] |
| Porosity of the tissue [$\varepsilon$] | 0.7 |
| Effective hydraulic conductivity [$\kappa^t$] | $10^{-11}$ [m$^2$] |
| Oxygen diffusivity in the culture media [$D^f$] | $10^{-9}$ [m$^2$s$^{-1}$] |
| Oxygen diffusivity in the tissue [$D^t$] | $10^{-10}$ [m$^2$s$^{-1}$] |

where B was the amount (nmole) of Nicotinamide adenine dinucleotide (NADH) generated between $T_{initial}$ and $T_{final}$, reaction time was the difference between $T_{initial}$ and $T_{final}$ and $V$ was the sample volume. All measurements were performed in triplicate in three independent experiments.

### 2.9. Histological, immunofluorescence and multiphoton imaging of 3D In-tube

3D In-tube was treated as previously reported (*Section 2.4*) for histological, immunofluorescence and SHG analyses. For immunofluorescent procedure, sections from the paraffin blocks were deparaffinized in xylene, treated with an incremental ethanol (100, 95 and 80% ethanol/double-distilled $H_2O$ [v/v]) and rehydrated in Dulbecco's PBS (pH 7.4). Antigens were unmasked by heat antigen retrieval with citrate buffer, pH 6.0 for 20 min. Slides were then blocked with 5% BSA (Sigma) and incubated with primary antibodies to Villin (1:200; Abcam), Claudin-1 (1:100; Abcam) and collagen IV (1:100, Abcam) overnight at 4 °C. After washing extensively, all slides were incubated with a 1:500 dilution of appropriate fluorescent secondary antibody (488 and 546 Alexa fluor, Thermo Fisher) at RT for 1 h. Slides were rinsed, and counterstained with DAPI (Sigma Aldrich) dilution ratio (1:10000 in PBS) for 10 min. Images of the stained samples were obtained using confocal laser scanning microscopy. For scanning electron microscopy (SEM) analysis, the 3D In-tube was fixed with 2.5% (v/v) glutaraldehyde in cacodylate buffer. Samples were washed twice in 100 mM cacodylate buffer, pH 7.2, for 10 min at RT. A second fixation in 1% (w/v) osmium tetroxide, buffered in 100 mM cacodylate, pH 7.2, was done overnight at 4 °C. Dehydration was carried out by gradually decreasing the water concentration and increasing the ethanol concentration (10%, 30%, 50%, 70%, 90%, 100% and 100% again, each step 30 min at RT). Samples were then treated with liquid carbon dioxide using a Critical Point Dryer (Emitech K850). Dried samples were mounted onto metal stubs using double-sided adhesive tape and then gold-coated using a sputter coater at 15 mA for 20 min. Coated samples were then examined by SEM (Leica S400).

### 2.10. Statistical analysis

All results were then statistically analyzed by the Student's *t*-test. To verify the presence of differences between the groups, we applied the analysis of variance. We reported the results of statistical tests as average ± SD. P-values $<0.05$ were considered statistically significant.

## 3. Results

### 3.1. Time evolution of InMyoFib-μTPs and its characterization

The InMyoFib-μTPs were obtained by seeding H-InMyoFib on GPMs, by partly modifying a previously described spinner flask culture [17,18]. Histological analysis showed the cells distribution over the microbeads surface indicating the H-InMyoFibs proliferation and collagen production in cell-GMP aggregates (InMyoFib-μTPs; Fig. 4A). High magnification H/E staining showed the neo-produced collagen matrix that connected the microbeads (Fig. 4A, inset). Morphological inspection and ECM deposition have been evaluated by confocal and multiphoton microscopy. The Fig. 4B reported the multichanneled images of InMyoFib-μTPs at 10 days of spinner culture highlighting cell's nuclei (blue), cell's cytoplasm (red) and unstained collagen (grey). Images showed the high amount of collagen around and into the cell—microbeads aggregates and the α-SMA signal indicated the 3D organization of H-InMyoFibs into cell—microbeads aggregates as well as the cell—microbeads interactions. We also reported the number of cells adhering to microbeads (cell/microbead ratio) as indication of the cell proliferation during the spinner culture at day 0, 3, 6 and 10 (Fig. 4C). The cell/microbeads ratio increased during culture time up to 100 cell*bead$^{-1}$. In addition, to evaluate the cell viability during microtissues production, LDH assay was performed. The results indicated that the viability of the InMyoFib-μTPs was well maintained, also thanks to the dynamic fluid condition that encourage nutrient exchange (Fig. 5A).

### 3.2. 3D In-tube stromal characterization

To obtain the 3D tubular stroma, a 3D planar stroma was rolled around a stainless steel cylindrical grid and inserted in the spinner flask. After 15 days in culture, the construct successfully assembled, retaining the 3D tubular shape (Video 1), the edges of the tissue sheet were completely fused by means of a healing-like process. The final shape mimics the intestine hollow with an inner diameter of 0.5 cm, a thickness of 1 mm and a length of 2.0 cm (Fig. 5B). We investigated the overall morphology of the 3D tubular stroma by confocal reconstruction and micro-CT analyses and the presence of matrix-associated protein, in particular the collagen components, by means of confocal and multiphoton microscopy. Immunofluorescence analysis highlighted the type III collagen (immature) and type I collagen (mature) signals in the lamina propria of the 3D tubular stroma (Fig. 5C). In particular, high amount of mature collagen (stained in red) compared with the immature one (stained in yellow) was revealed, resulting in a connective tissue that similarly to the native counterpart, is rich in collagen type I (Fig. 5C). We also highlighted the formation of the basement membrane by immunofluorescence staining of collagen IV. As reported in the high magnification image (Supplementary Fig. S1), a native and intact basement membrane was produced on 3D In-tube. Furthermore, images captured by micro-CT shows the macroscopic morphology of the tubular stroma with the lumen-like cavity (Fig. 5D) and confirm the presence of the H-InMyoFibs embedded into the neo-produced ECM (Fig. 5D, white arrowheads). Furthermore, the reconstruction of a slice of 3D tubular stroma at confocal multiphoton microscope is reported in Fig. 5E. The InMyoFib's cytoskeleton was stained with phalloidin (red) and the collagen fibres, detected by SHG imaging, were represented in grey. The images confirm a high amount of neo-produced collagen and show the myofibroblasts embedded in their own ECM, revealing a highly physiological environment that is fundamental to support intestinal epithelium morphogenesis [19]. Then, to evaluate the cell viability during InMyoFib-μTPs assembling and 3D tubular stroma formation, LDH (typical marker of damaged or injured tissues) release assay was used. Convective forces provided by stirring and medium flows [20] during the long-term

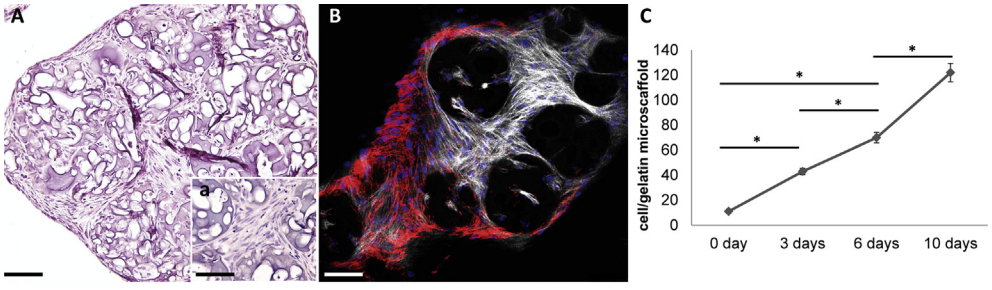


**Fig. 4.** Time evolution of the intestinal myofibroblasts microtissue precursors (InMyoFib-μTPs). A) Haematoxylin and eosin (H/E) staining of InMyoFib-μTPs at 10 days of dynamic culture, scale bar 200 μm; a) high magnification H/E staining, scale bar 50 μm; B) multichanneled image of InMyoFib-μTPs highlights cell's nuclei (blue), α-SMA (red) and unstained collagen (grey), scale bar 75 μm and C) graph of the cell/microbeads ratio at day 0, 3, 6 and 10. Data are presented as average ± SD; *$p<0.05$).

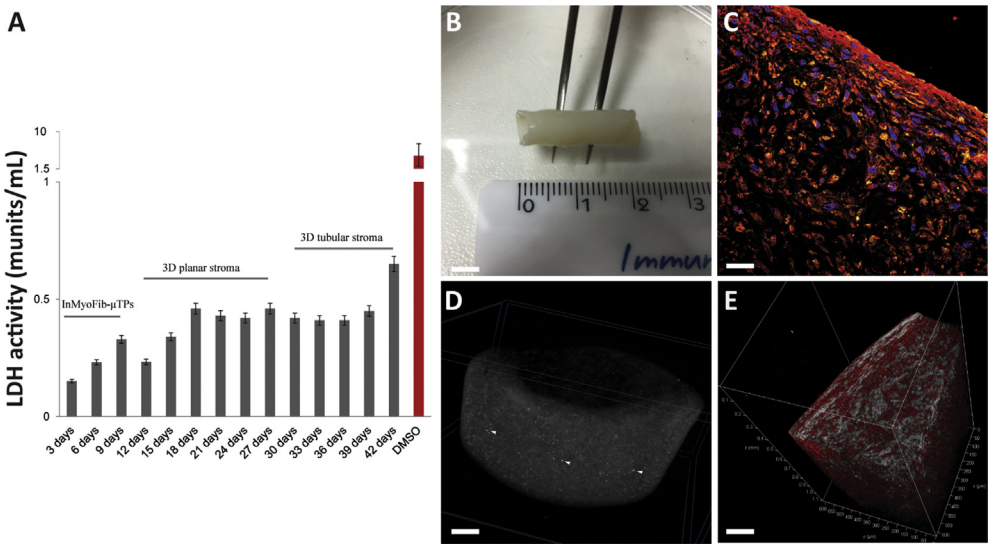


**Fig. 5.** 3D tubular stroma characterization. A and B) Evaluation of cell viability during long-term culture of human intestinal myofibroblasts (H-InMyoFibs) in InMyoFib-μTPs, 3D planar stroma and 3D tubular stroma by means of lactate dehydrogenase enzyme (LDH) release assay. Data are presented as average ± SD. C) Immunofluorescence analysis of 3D tubular stroma highlights the type III collagen (yellow) and type I collagen (red), scale bar 50 μm; D) microcomputed tomography reconstruction of the 3D tubular stroma evidences the lumen cavity, white arrowheads indicate the presence of the H-InMyoFibs embedded into the auto-produced extracellular matrix (ECM; white arrowheads), scale bar 0.6 cm and E) confocal multiphoton image of the 3D tubular stroma slice reconstruction highlights the H-InMyoFibs cytoskeleton (red) and collagen fibres (white), scale bar 200 μm

culture are necessary to induce the 3D planar stroma biosintering process and then to form the tubular stroma, guarantee the cell viability preservation (Fig. 5A). The resulting highly physiological environment was exploited to guide Caco-2 differentiation toward the absorptive and mucus-secretory phenotype.

Supplementary video related to this article can be found at https://doi.org/10.1016/j.mtbio.2019.100027.

### 3.3. 3D In-tube in microbioreactor

To develop the 3D In-tube, the Caco-2 cells were seeded on the luminal surface of the 3D tubular stroma. After cell seeding, the 3D In-tube was maintained in submerged conditions in static culture for 2 days to allow the formation of confluent intestinal epithelium. Then, the 3D In-tube was sealed with collagen gel and was placed into an on-made glass microbioreactor system, which had to be able to ensure both the stromal hydration and the epithelial cell differentiation during the ALI phase (Fig. 6A). Our results showed that the culture of Caco-2 cells on the inner surface of hollow 3D tubular stroma well resemble the relevant physiological microenvironment of enterocytes *in vivo* and thus stimulate the differentiation process of Caco-2 cells. CFD (Fig. 6B–D) was used to simulate fluid dynamic conditions and oxygen provision inside bioreactor to set the optimal flow rate to guarantee the cell's adhesion, collagen network assembly, velocity of nutrient supply and oxygen gradient. In the Fig. 6, the vectors and magnitude of velocity field (Fig. 6B), the magnitude and variation of pressure (Fig. 6C) and magnitude and variation of $O_2$ concentration (Fig. 6D) inside the bioreactor were reported. The flow rate was set at 8 mL/min (Re < 2100, laminar behaviour) that despite the presence of reaction occurring in the bioreactor environment guaranteed the $O_2$ concentration in the culture media in the same order of the initial concentration at the inlet such as 0.22 L mol/m$^3$. Fig. 6C showed that the pressure at the inlet was about 1.68 Pa, and the pressure at the outlet is very close to 0 Pa, so the pressure drop along z-direction in the bioreactor was very small. Fig. 6B showed that at inlet, a fully developed Poiseuille velocity profile was present with a maximum velocity of 0.0035 m/s. According to our plots, the maximum velocity of the fluid flow along the external wall of the 3D In-tube was 0.001 m/s, which is safe for cell viability according to literature [21].

### 3.4. Histological, immunofluorescence and multiphoton imaging of 3D In-tube

We also compared the morphological features of the 3D In-tube cultured in static or dynamic conditions. Histological analyses (Fig. 7A and B) highlighted that besides to the presence of the curvy surface because of+ the tubular geometry of the stroma, the presence of the peristalsis-like movement induced the production of stromal protrusions and highly polarized epithelial cells with microvilli-covered surface in the hollow lumen of the 3D In-tube (Fig. 7A and B). In contrast, when the ALI culture was performed under static conditions, a flat lumen surface

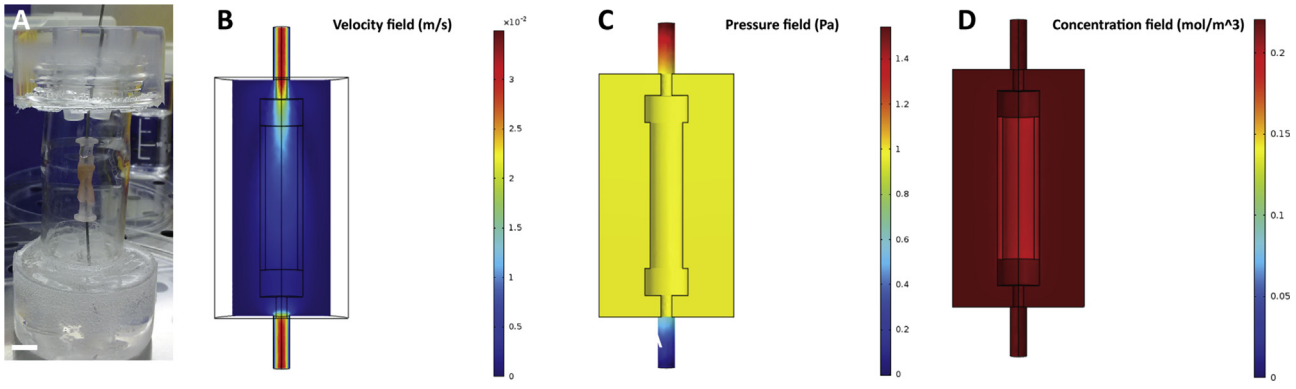


**Fig. 6.** CFD study of bioreactor system for ALI culture of Caco-2 cells. A) Bioreactor systems for dynamic epithelial cells culture in ALI conditions, scale bar 1 cm; B) velocity field in the bioreactor system at a flow rate of 8 mL/min; C) pressure field in the bioreactor system at a flow rate of 8 mL/min showed a slight pressure drop along z-direction and D) oxygen concentration field in the bioreactor system working at a flow rate of 8 mL/min.

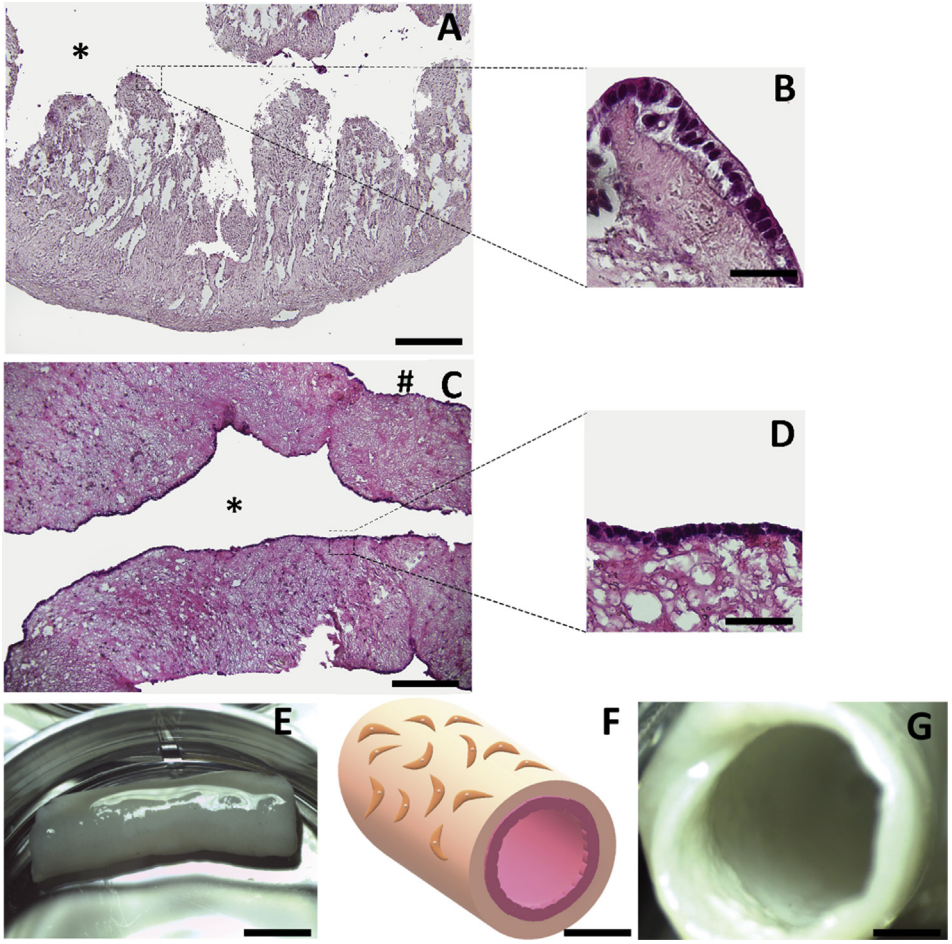


**Fig. 7.** Histochemical analysis of 3D In-tube under static or dynamic ALI culture. A and B) H/E staining of 3D In-tube in dynamic condition showed curvy lumen surface with stromal protrusions and highly polarized epithelial cells (F, scale bar 200 μm; G, scale bar 50 μm); * lumen side, # serosal side; C and D) H/E staining of 3D In-tube in static condition showed flat lumen surface with a single Caco-2 layer (D, scale bar 200 μm; E, scale bar 50 μm); E) stereo microscope observation of 3D In-tube, scale bar 0.8 cm; F) schematic cartoon of the 3D In-tube with H-InMyoFibs into the neo-produced ECM and Caco-2 cells in the lumen side, scale bar 0.25 cm and G) picture captured at stereo microscope shows the lumen of the 3D In-tube featured by a corrugated surface, scale bar 0.2 cm;

with a single Caco-2 layer overlying the stroma was found (Fig. 7C and D). Ultrastructural micrograph of CaCo-2 seeded on 3D In-tube in both static and dynamic conditions showed the higher production of microvilli structures on the free surface of the epithelial cells in dynamic compared with the static conditions (Supplementary Fig. S2A and B). Furthermore, Fig. 7B displayed the schematic design of the 3D In-tube with H-InMyoFibs embedded into the neo-produced ECM and Caco-2 cells seeded in the lumen side. Stereo microscope observation of the outer flat surface (Fig. 7E) and inner (Fig. 7G) lumen of the 3D In-tube confirmed the presence of the corrugated inner surface (Fig. 7G, Video 2), because of the presence of the stromal protrusion covered by enterocyte-like epithelial cells that mimic the *in vivo* villous structure and the high absorptive surface of the mucosa. To further evaluate the phenotype of the cells in the lumen side of the 3D In-tube cultured in the micro-bioreactor, immunofluorescence microscopy was performed to detect the expression of a differentiation marker in intestinal epithelium. Fully polarized epithelial cells were also confirmed by SEM (Fig. 8A and B) acquisition indicating that the free surfaces of the apical cells were covered by the high packing microvilli with a continuous brush borders across the cells (Fig. 8B, black arrowheads). Ultrastructural analysis also reports the mucus secretion in the lumen side of the 3D In-tube, so indicating the presence of the mucus-producing cell phenotypes (Fig. 8B, white arrowheads and b inset). On the other hand, SEM studies of the 3D In-tube model at stromal level revealed the presence of the neo-produced collagen (Fig. 8A) and the images at higher magnification highlight the collagen fibres organized in bundles (Fig. 8A, inset). The expression of Villin, a major component of the inner surface of the enterocyte (Fig. 8C and c inset), suggested that the 3D bioreactor system was suitable for differentiation of the intestinal tissues. We also demonstrated the formation of tight paracellular barrier and a continuum brush border on the apical surface of the epithelial cells. The appropriate cell polarization suggests that 3D In-tube can be a useful model for drug permeability prediction improving the efficacy of drug screening process. In this regard, we evaluate the expression of the Claudin-1, a tight junction protein expressed in epithelial tissues that play important roles in cell polarity and adhesion (Fig. 8D and d inset).

Supplementary video related to this article can be found at https://doi.org/10.1016/j.mtbio.2019.100027

## 4. Discussion

This study attempted to develop a 3D tubular intestine model with morphological, biological and functional properties mimicking the native small intestine. As we previously demonstrated, H-InMyoFibs proliferated and synthesized *de novo* ECM onto GPMs resulting in functional building blocks able to be assembled in a bioreactor chamber producing a 3D intestinal lamina propria [17,18]. We further demonstrated the effect of composition and topography of such 3D intestinal lamina propria in promoting intestinal epithelium morphogenesis *in vitro*. However, beyond the multilayered structure of epithelium, the tubular shape and the peristalsis motility of the small intestine are key structural features for the physiological functions of this organ, especially for the movement of luminal content. Therefore, here, we challenge the Caco-2 cells to differentiate on the lumen side of a 3D tubular stroma by designing a handy microbioreactor able to perform ALI culture on a curvy surface in dynamic conditions mimicking the peristaltic-like motion. First of all, we used a modular tissue assembling approach to fabricate the tubular intestinal stroma composed by H-InMyoFibs embedded in their own ECM.

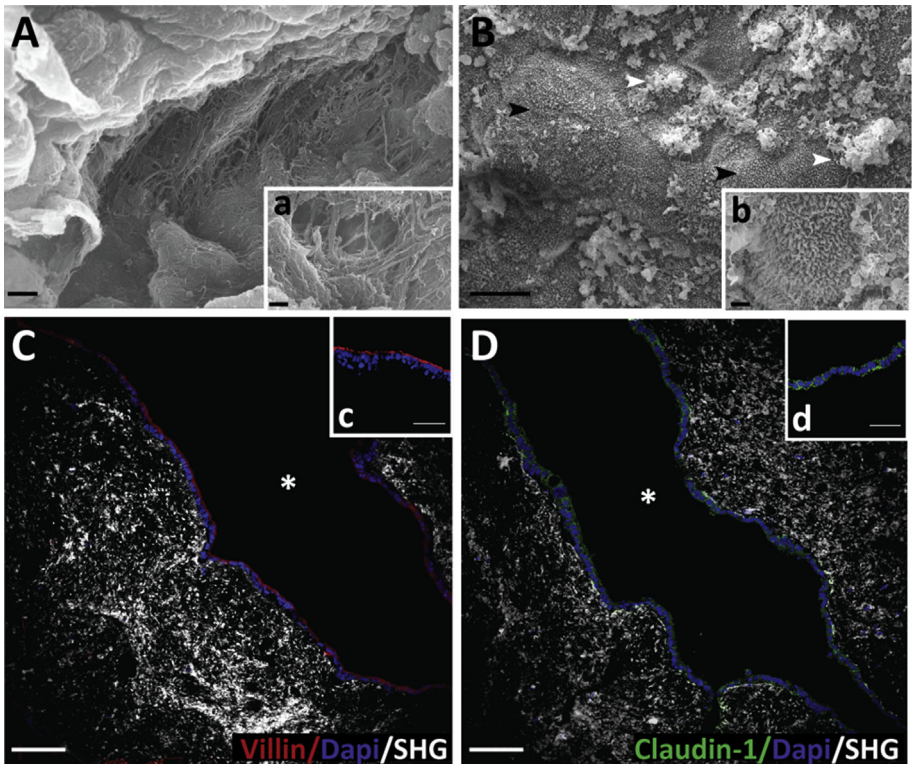


**Fig. 8.** Ultrastructural and immunofluorescence of the 3D In-tube after dynamic ALI culture and peristaltic-like motion. A, a) Scanning electron microscope acquisitions showed the serosal side of the 3D In-tube model featured by neo-produced collagen and bundles of collagen fibres (A, scale bar 10 μm; a, scale bar 1 μm); B, b) scanning electron microscope acquisitions show the intestinal epithelium in the lumen side. In particular, free surfaces of apical cells are shown with high-packing microvilli (black arrowheads) and mucus (white arrowheads) (B, scale bar 10 μm; b, scale bar 1 μm); C, c) immunofluorescence analysis of 3D In-tube for epithelial differentiation marker highlights the Villin (red), Dapi (Blue) and SHG (white) (C, scale bar 75 μm; c, scale bar 25 μm) and D, d) Claudin-1 (green), Dapi (Blue) and SHG (white) (D, scale bar 75 μm; d, scale bar 25 μm).

As it is well known, the ECM is a highly dynamic structure and its synthesis is markedly dependent on dynamic culture conditions and 3D environment [18]. As expected, the H-InMyoFibs in 3D tubular stroma are embedded in the neo-produced ECM subjected to a continuous remodelling that provides a suitable microenvironment for cell growth. We investigated the overall morphology of the 3D tubular stroma by confocal reconstruction and micro-CT analyses and the presence of matrix-associated protein, in particular the collagen components, by means of confocal and multiphoton microscopy. As predictable, a high production of ECM components was found leading to an ECM composition similar to the native small intestinal mucosa that is fundamental to support intestinal epithelium morphogenesis. Recapitulating the morphology and the macromolecular composition of the intestinal stromal ECM has important implications in gut bioengineering that is moving from cell-free tissue scaffolds toward gastrointestinal constructs with native physiological functions. The tubular models currently used have their strengths and limitations, the appropriateness of the model depends on which features and cellular behaviours are recapitulated *in vitro*. In particular, for the development of 3D tubular-shaped model, the choice of the ECM-equivalent and the impact of long-term co-culture on cell behaviour greatly affect the outcome [22]. Our results demonstrate the production of a reliable 3D In-tube that maintains cell viability during the long-term culture as confirmed by LDH assay that showed no damage of the H-InMyoFibs from the beginning of the InMyoFib-μTPs to the 3D tubular stroma formation. More importantly, we demonstrated the suitability of the 3D tubular stroma in hosting a well-polarized intestinal epithelium by seeding and culture Caco-2 cells on its inner surface. In addition, when the fluid flow and the peristaltic-like motion were applied, the spontaneous formation of villus-like protrusion was found with spatial differentiation of the intestinal epithelial cells in enterocyte-like as well as mucus-producing—like cells, resulting in enhanced absorbing surface area. The use of the peristaltic pump to mimic *in vivo* fluid mechanical environments has been previously reported in microfluidic devices for inducing a pulsatile liquid flow on 2D endothelial cells layer [23]. In our study, we used peristaltic pump, by modulating the flow rate, for reproducing the intestinal peristalsis movement [17] on the external wall of 3D In-tube. In particular, during dynamic culture, rotation of the peristaltic pump generates a slight pressure fluctuation that induces a coordinated contraction stress, thus providing Caco-2 cells with the proper physical signals (i.e. mechanical stress and distribution of chemical factors) that promote the formation of villus-like protrusion. The peristaltic pump emulates the biological process of peristalsis-like stimulus, in which material is moved through the oesophagus or other anatomical passage by the contraction of smooth muscle in rhythmic waves [24]. Moreover, the dynamic fluid flow conditions during ALI culture, assured, as confirmed by CFD simulation, the oxygen supply is necessary to cell viability. We assessed the functionality of the intestinal epithelium developed in the lumen side of the 3D In-tube subjected to peristaltic-like motion by investigating the production of a native and intact basement membrane in terms of collagen IV production as well as the paracellular tight junction production by immunostaining of claudin-1 and brush border development on the apical surface of the epithelial cells by immunofluorescence staining of villin. It is noteworthy that the intestinal epithelium acts as front lines barrier of defence against luminal pathogens, toxins and antigens, from the luminal environment into the mucosal tissues and circulatory system [25]. Apical tight junction proteins and basal lamina maintain the epithelial barrier function and control the paracellular permeability [26]. Hence, the appropriate cell polarization indicates that our model is useful to drug permeability prediction helping drug screening process. In addition, the detection of the mucus production, analyzed by ultrastructural analysis, further confirmed the barrier function on the luminal side of 3D In-tube. The possibility to induce a peristaltic-like movement to a physiologically relevant model such as 3D In-tube paves the way for a use of the system to evaluate chyle absorption and metabolism in controlled conditions and also for studying the peristaltic-related pathologies. Moreover, 3D In-tube, thanks to its self-standing capability because of the auto-produced collagenous components, could satisfy clinical demand for personalized intestinal tissue grafts, overcoming current problems such as reduction in mucosal surface area and donor tissue rejection [2]

or surgical intervention-resection of the diseased gut segment for the treatment of intestinal failure of short bowel syndrome.

## 5. Conclusion

In conclusion, we designed a custom-made microbioreactor system that supports the ALI culture of the bioengineered 3D In-tube and induce peristalsis-like stimuli. We analyzed the H-InMyoFibs viability into the auto-produced connective tissue and also the key features of the intestinal epithelial cells (epithelial polarization, differentiation and barrier function) cultured into the lumen side of the 3D In-tube. We strongly believe that the proposed system because of its luminal accessibility could find future applications to study the dynamic host–microbiome–intestinal interactions in a long-time culture, helping in understanding the food absorption under peristaltic movement.

## Declaration of competing interest

The authors declare that they have no known competing financial interests or personal relationships that could have appeared to influence the work reported in this paper.

## Acknowledgements

The authors thank Dr. Valentina Mollo for her precious support to the SEM and micro-CT analyses and Dr. Fabio Formiggini for his support in the confocal reconstruction of 3D In-tube.

## Appendix A. Supplementary data

Supplementary data to this article can be found online at https://doi.org/10.1016/j.mtbio.2019.100027.

## References

[1] W. Zhou, Y. Chen, T. Roh, Y. Lin, S. Ling, S. Zhao, J.D. Lin, N. Khalil, D.M. Cairns, E. Manousiouthakis, M. Tse, D.L. Kaplan, Multifunctional bioreactor system for human intestine tissues, ACS Biomater. Sci. Eng. 4 (1) (2018) 231–239.
[2] J. Basu, T.A. Bertram, Regenerative medicine of the gastrointestinal tract, Toxicol. Pathol. 42 (1) (2014) 82–90.
[3] R.M. Day, Epithelial stem cells and tissue engineered intestine, Curr. Stem Cell Res. Ther. 1 (1) (2006) 113–120.
[4] M.W. Tibbitt, K.S. Anseth, Hydrogels as extracellular matrix mimics for 3D cell culture, Biotechnol. Bioeng. 103 (4) (2009) 655–663.
[5] J.L. Drury, D.J. Mooney, Hydrogels for tissue engineering: scaffold design variables and applications, Biomaterials 24 (24) (2003) 4337–4351.
[6] M. Ehrbar, A. Sala, P. Lienemann, A. Ranga, K. Mosiewicz, A. Bittermann, S.C. Rizzi, F.E. Weber, M.P. Lutolf, Elucidating the role of matrix stiffness in 3D cell migration and remodelling, Biophys. J. 100 (2) (2011) 284–293.
[7] D. Huh, G.A. Hamilton, D.E. Ingber, From 3D cell culture to organs-on-chips, Trends Cell Biol. 21 (12) (2011) 745–754.
[8] R.S. Choi, M. Riegler, C. Pothoulakis, B.S. Kim, D. Mooney, M. Vacanti, J.P. Vacanti, Studies of brush border enzymes, basement membrane components, and electrophysiology of tissue-engineered neointestine, J. Pediatr. Surg. 33 (7) (1998) 991–996, discussion 996-7.
[9] T.C. Grikscheit, A. Siddique, E.R. Ochoa, A. Srinivasan, E. Alsberg, R.A. Hodin, J.P. Vacanti, Tissue-engineered small intestine improves recovery after massive small bowel resection, Ann. Surg. 240 (5) (2004) 748–754.
[10] X. Deng, G. Zhang, C. Shen, J. Yin, Q. Meng, Hollow fiber culture accelerates differentiation of Caco-2 cells, Appl. Microbiol. Biotechnol. 97 (15) (2013) 6943–6955.
[11] X. Wang, Q. Jiao, S. Zhang, Z. Ye, Y. Zhou, W.S. Tan, Perfusion culture-induced template-assisted assembling of cell-laden microcarriers is a promising route for fabricating macrotissues, Biotechnol. J. 9 (11) (2014) 1425–1434.
[12] J.H. Sung, J. Yu, D. Luo, M.L. Shuler, J.C. March, Microscale 3-D hydrogel scaffold for biomimetic gastrointestinal (GI) tract model, Lab Chip 11 (3) (2011) 389–392.
[13] P.H. Dedhia, N. Bertaux-Skeirik, Y. Zavros, J.R. Spence, Organoid models of human gastrointestinal development and disease, Gastroenterology 150 (5) (2016) 1098–1112.
[14] A.L. Bredenoord, H. Clevers, J.A. Knoblich, Human tissues in a dish: I research and ethical implications of organoid technology, Science 355 (6322) (2017).
[15] V. De Gregorio, G. Imparato, F. Urciuolo, P.A. Netti, 3D stromal tissue equivalent affects intestinal epithelium morphogenesis in vitro, Biotechnol. Bioeng. 115 (4) (2018) 1062–1075.
[16] V. De Gregorio, G. Imparato, F. Urciuolo, P.A. Netti, Micro-patterned endogenous stroma equivalent induces polarized crypt-villus architecture of human small intestinal epithelium, Acta Biomater. 81 (2018) 43–59.
[17] K.K. Lee, H.A. McCauley, T.R. Broda, M.J. Kofron, J.M. Wells, C.I. Hong, Human stomach-on-a-chip with luminal flow and peristaltic-like motility, Lab Chip 18 (20) (2018) 3079–3085.
[18] V. De Gregorio, G. Imparato, F. Urciuolo, M.L. Tornesello, C. Annunziata, F.M. Buonaguro, P.A. Netti, An engineered cell-instructive stroma for the fabrication of a novel full thickness human cervix equivalent in vitro, Adv. Healthc. Mater. 6 (11) (2017).
[19] L. Le Guen, S. Marchal, S. Faure, P. de Santa Barbara, Mesenchymal-epithelial interactions during digestive tract development and epithelial stem cell regeneration, Cell. Mol. Life Sci. 72 (20) (2015) 3883–3896.
[20] B.D. Ratner, Biomaterials Science: an Introduction to Materials in Medicine, third ed., Elsevier/Academic Press, Amsterdam ; Boston, 2013.
[21] B. Corrado, V. De Gregorio, G. Imparato, C. Attanasio, F. Urciuolo, P.A. Netti, A three-dimensional microfluidized liver system to assess hepatic drug metabolism and hepatotoxicity, Biotechnol. Bioeng. 116 (5) (2019) 1152–1163.
[22] I. Holland, J. Logan, J. Shi, C. McCormick, D. Liu, W. Shu, 3D biofabrication for tubular tissue engineering, Biodes Manuf. 1 (2) (2018) 89–100.
[23] C.K. Byun, K. Abi-Samra, Y.K. Cho, S. Takayama, Pumps for microfluidic cell culture, Electrophoresis 35 (2–3) (2014) 245–257 [20] J. Berg, T. Dallas, Peristaltic Pumps, 2015, pp. 2693-2701.
[24] J. Berg, T. Dallas, Peristaltic Pumps, 2015, pp. 2693–2701.
[25] M. Albert-Bayo, I. Paracuellos, A.M. Gonzalez-Castro, A. Rodriguez-Urrutia, M.J. Rodriguez-Lagunas, C. Alonso-Cotoner, J. Santos, M. Vicario, Intestinal mucosal mast cells: key modulators of barrier function and homeostasis, Cells 8 (2) (2019).
[26] C. Chelakkot, J. Ghim, S.H. Ryu, Mechanisms regulating intestinal barrier integrity and its pathological implications, Exp. Mol. Med. 50 (8) (2018) 103.